
Sensing properties of pellets based on mesoporous structures of ZnO

R. Herrera-Rivera, A. M. Pineda, M. de la L. Olvera and A. Maldonado

MRS Advances / *FirstView* Article / April 2016, pp 1 - 7
DOI: 10.1557/adv.2016.267, Published online: 19 April 2016

MRS Advances © 2016 Materials Research Society
DOI: 10.1557/adv.2016.267

Sensing properties of pellets based on mesoporous structures of ZnO

R. Herrera-Rivera[1], A. M. Pineda[1], M. de la L. Olvera[1,2] and A. Maldonado[1,2]
[1] Programa de Doctorado en Nanociencias y Nanotecnología, Centro de Investigación y de Estudios Avanzados del Instituto Politécnico Nacional. México, D.F., MEXICO
[2] Departamento de Ingeniería Eléctrica, Centro de Investigación y de Estudios Avanzados del Instituto Politécnico Nacional. México, D.F., MEXICO

ABSTRACT

Mesoporous zinc oxide nanopowders were synthesized by the homogenous precipitation method. Zinc acetate dissolved in water, at different molar concentrations, was used as Zn precursor, whereas ammonium carbonate ($(NH_4)_2CO_3$) and ammonium hydroxide (NH_4OH) were used to prepare the precipitant solutions. The precipitated powders were dried in a conventional drying chamber at 100°C for 1 h, and then calcined at 400°C during 2 h. Crystal structure of powders was determined by X-ray Diffraction (XRD), and the crystallite sizes were calculated from Scherrer's formula. Morphological characteristics (size and shape) were analyzed from Scanning Electron Microscopy (SEM). The surface area and the pore volume were obtained from BET analysis. The hexagonal wurtzite phase was corroborated in all synthesized powders, irrespective of the synthesis conditions. From SEM micrographs different structures, depending on the experimental routes, were observed. In order to test the sensing properties of the ZnO nanopowders, 10 mm diameter pellets were manufactured and then measured in a propane (C_3H_8) atmosphere at different gas concentrations and temperatures. Pellets processed from ZnO powders at 0.05, 0.35, and 0.5 M presented the highest sensitivity, 413, 532, at 300°C and 500 ppm of C_3H_8.

INTRODUCTION

Different metal oxide semiconductors (MOS) have been used as chemo-resistive sensors, for example: SnO_2, TiO_2, In_2O_3, and ZnO among others [1]. Zinc oxide is n-type native semiconductor, chemically stable in wurtzite phase, with a large bandgap, around 3.37 eV at room temperature. In thin film form, present a high optical transparency, as well as a high electrical conductivity when it is doped with the adequate impurities [2-3]. These physical properties make ZnO a good candidate for different optoelectronic applications, for example as antireflective and piezoelectric layers [4], light emission diodes (LEDs) [5], thermal mirrors [6], liquid crystal displays (LCDs) [7], and chemical gas sensors [8], among others.

Additionally, ZnO is used in pharmaceuticals and/or cosmetics applications like sunscreen protectors, acne treatment, or as antiseptic in ointments [9].

According to the required properties, ZnO thin films can be processed from different synthesis techniques, such as pyrolysis spray [10], sputtering [11], pulsed laser deposition [12], and sol-gel [13]. However for sintering ZnO powders only few methods have been reported in the literature, among these is the homogeneous precipitation method [14]. This method is a simple and low cost route; nevertheless it conduces to a high quality material.

The study of nanostructures with different morphologies, dimension and porosity has attracted the interest of researchers in the area of gas sensors because porous morphologies favor

increased gas sensitivity in devices. The main advantages of these types of structures include the large surface, less agglomerated structures, and slow electron/hole recombination rate [3, 15-17].

There are two goals for this work: the first is to analyze the structural and morphological properties of mesoporous zinc oxide (ZnO) nanopowders prepared by the homogeneous precipitation method; and the second one is to manufacture pellets from ZnO nanopowders in order to study their sensing properties in a propane (C_3H_8) atmosphere at different concentrations and operation temperatures.

EXPERIMENT

ZnO powders were synthesized from starting solutions prepared from zinc acetate dihydrate [$Zn(CH_3COO)_2{\cdot}2H_2O$] at different molar concentrations, namely, 0.05, 0.35, and 0.5 M, and ammonium carbonate [$(NH_4)_2CO_3$] and ammonium hydroxide (NH_4OH) as precipitant agents. For preparing the starting solutions with ammonium carbonate, a mixture of de-ionized water and ethanol was employed, whereas for ammonium hydroxide only water was used. The solution was prepared at temperatures of 30 or 70°C under constant magnetic stirring, 100 or 500 rpm, and two stirring times, 60 or 120 min. The experimental conditions are presented in Table I.

It should be mentioned that, in this work are reported only three samples, because the main intention is to analyze the effect of the ZnO structure type on the sensing characteristics of the pellets. In this respect, these three samples correspond to the synthesized powders with the smallest particle size, optimized from an 18 experiments array, which was designed according to the Taguchi's technique [18].

Table I. Preparation conditions of ZnO nanopowders

Sample	Precursor solution		Precipitating solution		Operating condition		
	Solvent (60 ml of H_2O)	Molarity [M]	Precipitant	Solvent (100 ml)	Stirring rate (rpm)	Stirring time (min)	Temperature (°C)
A	$Zn(CH_3COO)_2{\cdot}2H_2O$	0.05	$(NH_4)_2CO_3$	H_2O	500	60	30
B		0.35	NH_4OH			120	70
C		0.5	$(NH_4)_2CO_3$	CH_3-CH_2-OH	100		

All starting solutions were centrifuged in an Eppendorf Model 5430 centrifuge, at 4500 rpm for 6 min; resulting a white solid paste that was recovered and then washed thrice in 45 ml of methanol. Subsequently, the resultant paste was dried at 100°C for 1 h, and finally, the dried powders were calcined at 400°C for 2 h, in an air atmosphere, in order to remove any residual organic material.

From calcined powders, 10 mm diameter pellets were manufactured with a stainless steel die, by using a hydraulic pressing machine (ITAL Mexicana) at 5 Ton for 10 min. For electrical measurements two ohmic contacts were outlined onto the pellets by using high purity silver paint (from SPI).

A PANalytical Model X'PERT-PRO diffractometer, operating in 2θ mode and using the Cu-Kα1 radiation (λ=1.54060 Å) was used to analyze the structural properties. The spectra were taken in the 30-80° range. The morphological properties were studied by a Scanning Electron Microscopy (SEM) with an AURIGA equipment, operated at 5.00 kV for sample A and 2.00 kV for samples B and C.

The sensing measurements were carried out in a sealed quartz chamber, containing propane gas (C_3H_8) at different concentrations (1, 5, 50, 100, 200, 300, 400, and 500 ppm) and operation temperatures of 100, 200, and 300°C. The electrical resistance measurements were obtained with a Keithley 2001 multimeter. The gas concentration into the quartz chamber was indirectly controlled by pressure measurements using a TM20 Leybold detector. The sensitivity, S, was calculated as the relative ratio of the electrical resistance measured in a normal atmosphere, R_a, and in propane, R_g. See equation 1.

$$S = [R_a - R_g] / R_g \quad (1)$$

In order to analyse the effect of the surface area of the ZnO nanopowers on the sensing properties, the specific surface area was measured by 12-point nitrogen adsorption (Brunauer–Emmett–Teller (BET): Micromeritics, Gemini 3240) after degassing the powder at 150°C for 2 h in nitrogen.

RESULTS AND DISCUSSION

Structural and morphological properties of ZnO nanopowders

The XRD patterns of the ZnO nanopowders are shown in figure 1, all diffractograms revel a high crystalline hexagonal wurtzite phase of ZnO, according to the JCPDS 00-005-0664 card. The average particle sizes of the different ZnO samples were calculated from the (101) peak by using Scherrer's equation,

$$D_{hkl} = c\lambda / \beta cos\theta \quad (2)$$

Where, c is a constant (~0.89), λ is the wavelength of the Cu-α radiation (0.154060 nm), θ is the Bragg´s diffraction angle in degrees, and β is the line width at half peak intensity in radians [16]. The crystallite sizes estimated were around 42, 52 and, 32 nm, for samples A, B, and C, respectively. In Table II are reported these data.

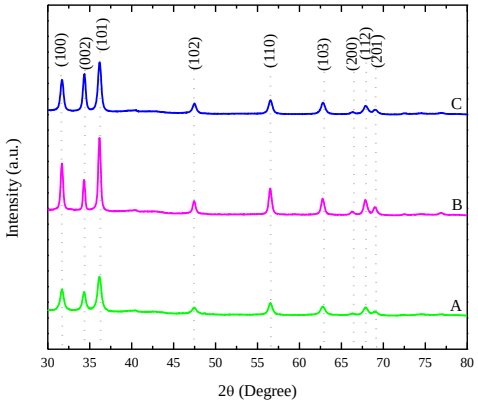

Figure 1. Representative XRD patterns of ZnO nanopowders calcined at 400°C for 2 h.

Figures 2-4 show the morphological analysis of the three samples; so, micrographs with different magnifications are presented. Figure 2a shows the panoramic image of ZnO nanorods-like self-assembly with transversal sections and lengths around 212 and 2000 nm, respectively. Additionally, some agglomerates of small spherical particles are also observed. Figure 2b, shows a close up of figure 2a, where it can be observed that bars are completely conformed or covered of spherical nanoparticles, with an average diameter size, around 28 nm. The self-assembly of

the rods could be generated by the dipole-dipole interaction between nanograins initially oriented along the c-axis, as was stated previously by Jiaheng Wang et al. [19].

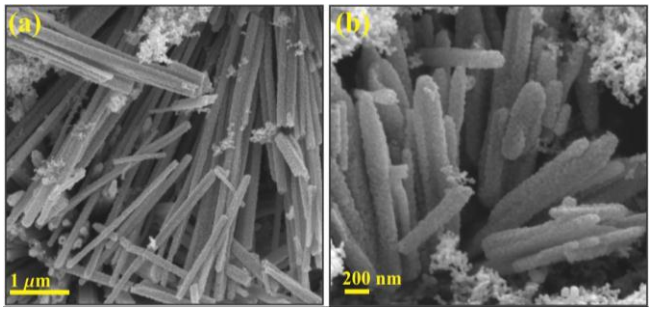

Figure 2. (a) SEM image of sample A.

Figure 3 shows the SEM images of sample B. The image 3a shows a wide area of sample, where it can be observed elongated particles with an average length and diameter around 675 and 370 nm, respectively. The features seems to be constituted from lots of tiny rounded nanoparticles, exhibiting a like nanoflowers morphology, as can be observed in the close up in figure 3b.

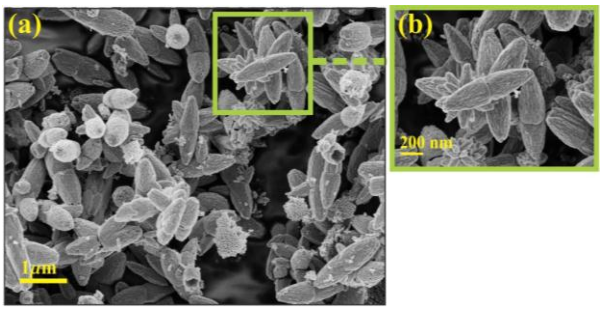

Figure 3. SEM image of sample B. (a) Panoramic view, and (b) close up of a ZnO like-nanoflower.

ZnO nanopowders obtained in sample C exhibits a mesoporous spherical morphology. Figure 4a shows a SEM micrograph of a large area. In this image, it can be observed a spherical mesoporous structure with nanoparticles of different diameters estimated from the ImageJ software; the diameter magnitudes oscillated between 439 and 1337 nm. A close up of mesoporous spherical ZnO nanostructures are presented figure 4b. From this image it can be evidenced that, a self-assembly from smaller spherical particles, with an average size of ~ 23 nm, was formed.

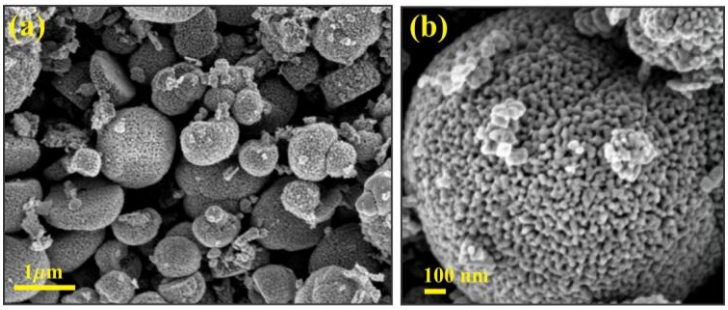

Figure 4. SEM images of ZnO nanopowders, sample C.

Gas sensing properties of ZnO pellets

Figure 5 shows the graphs of sensitivity versus propane concentration of ZnO pellets manufactured from nanopowders A, B, and C. From plots of figure 5 it is evident that, the sensitivity registered at 100°C is very small and almost constant with the propane concentration variation; this result is due to at these conditions there is not enough energy to activate the oxygen desorption. Beyond 200°C the gas sensitivity increases in all cases, this is due to desorption of the different oxygen species (O^{2-}, O^{-}) on the surface, initially adsorbed, increases. This desorption is improved at higher temperatures, and consequently the sensitivity is increased with the operation temperature, as can be observed from plots 5a-c. In the case of pellet processed from powder B, it presented the lowest sensitivity magnitudes, irrespective of operation temperature, as compared with pellets fabricated from powders A and C, this result is associated to the compactness and size of particles, besides presenting the lowest pore volume, according to the BET analysis results (Table II). Pellets manufactured from powders A and C show higher sensitivities, figures 5a and c, despite the area of powders is closely similar in the three samples, 16.68-19.97 m^2g^{-1}, as was corroborated from BET analysis (Table II). From this result, it could be elucidated that samples with smaller particle size, A and C, present higher catalytic activity to increase the adsorption of oxygen species, since samples A and C showed the lowest values, around 28 and 23 nm, respectively. Additionally, according to the morphologies presented in samples A and C it can be considered that pellets could present a better connectivity among the particles, leading to a better electrical conduction, therefore the sensing response is different, in despite of presenting similar areas and pore volume, as is shown in Table II.

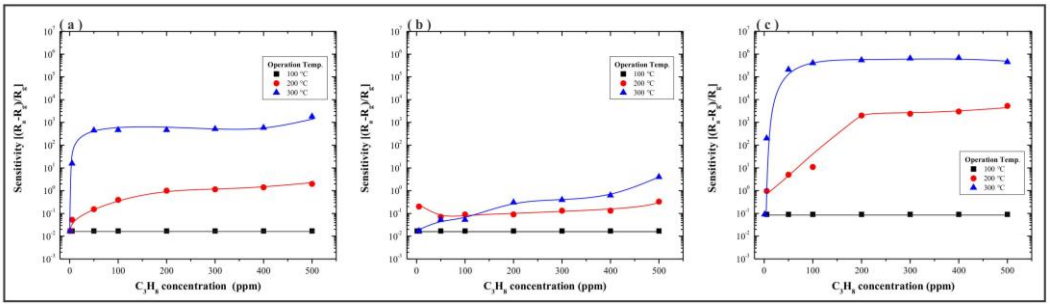

Figure 5. Sensitivity as a function of C_3H_8 concentration at different operation temperatures, for the pellets processed from nanopowders, A, B and C.

Table II. BET surface areas, total pore volume, and crystallite sizes of calcined samples

Sample	Crystal size (nm)	BET area (m^2g^{-1})	Total pore volume / cm^3g^{-1}
A	42	19.97	0.025
B	52	18.27	0.022
C	32	16.68	0.231

CONCLUSIONS

In summary, three different mesoporous nanostructure of ZnO were synthetized by the homogeneous precipitation method. Spherical nanoparticles for the samples A and C, with a

diameter ranging between 23 to 28 nm, were synthetized from ammonium carbonate as precipitant agent; these nanoparticles showed a self-assembly rod-like and mesoporous spherical. The rod-like and the mesoporous spherical ZnO nanopowders showed good sensitivity in the presence of propane at 200 and 300°C. The best sensitivity was presented in mesoporous spheres, sample C, which was higher than six orders of magnitude at 300°C. No significant sensitivity changes to propane gas were presented in flower-like nanostructures, at least under the conditions described in this work. From BET analysis it was encountered that closely similar characteristics are presented in the three samples analyzed, then the surface area and porosity cannot be associated as the direct cause of the different behaviors in the sensing response, at least in the samples studied in this work. From results obtained in this work it can be concluded that, ZnO nanopowders synthesized from the homogeneous precipitation method can be potentially considered for gas sensing applications.

ACKNOWLEDGMENTS

The authors appreciate the support received from D. Bahena (TEM analysis) and A. Ángeles (SEM analysis) from the Advanced Laboratory of Electron Nanoscopy from CINVESTAV, A. Tavira-Fuentes (X-ray characterization), and M. Tellez-Cruz (BET analysis). R. Herrera-Rivera also acknowledges the financial support received from CONACyT through the PHD scholarship. This work was partially supported by CONACYT, through project number 155996.

REFERENCES

1. M. Hijiri, L. El Mir, S.G. Leonardi, A. Pistone, L. Mavilia, and G. Neri. *Al-doped ZnO for highly sensitive CO gas sensors*. Sensors and Actuators B, **196**, (2014), pp. 413-420.
2. Shoou-Jinn Chang, Ting-Jen Hsueh, I-Cgerng Chen, and Bohr-Ran Huang. *Highly sensitive ZnO nanowire Co sensors with the adsorption of Au nanoparticles.* IOP Publishing Nanotechnology **19** (2008) **175502**.
3. Shaohong Wei, Shaomei Wang, Yan Zhang, and Meihua Zhou. *Different morphologies of ZnO and their ethanol sensing property.* Sensors and Actuators B, **192**, (2014), pp. 480-487.
4. O Kluth, B Rech, L Houben, S Wieder, G Schöpe, C Beneking, H Wagner, A Löffl, and H.W Schock. *Texture etched ZnO:Al coated glass substrates for silicon based thin film solar cells.* Thin Solid Films, **351**, (1999), pp. 247–253.
5. Jiming Bao, Mariano A. Zimmler, Federico Capasso, Xiaowei Wang, and Z. F. Ren. *Broadband ZnO Single-Nanowire Light-Emitting Diode.* Nano Letters, **6**, (2006), pp. 1719–1722.
6. Zhong Lin Wang. *Zinc oxide nanostructures: growth, properties and applications.* Journal of Physics: Condensed Matter. (2004), pp. 829-831.
7. Byeong-Yun Oh, Min-Chang Jeong, Tae-Hyoung Moon, Woong Lee, Jae-Min Myoung, Jeoung-Yeon Hwang, and Dae-Shik Seo. *Transparent conductive Al-doped ZnO films for liquid crystal displays.* J. Appl. Phys. **99**, (2006), **124505**.
8. Hailin Tian, Huiqing Fan, Hui Guo, and Na Song. *Solution-based synthesis of ZnO/carbon nanostructures by chemical coupling for high performance gas sensors*. Sensors and Actuators B: Chemical, **195**, (2014), pp. 132-139.

9. Majid Darroudi, Zahra Sabouri, Reza Kazemi Oskuee, Ali Khorsand Zak, Hadi Kargar, and Mohamad Hasnul Naim Abd Hamid. *Green chemistry approach for the synthesis of ZnO nanopowders and their cytotoxic effects.* Ceramics International, **40**, (2014), pp. 4827-4831.
10. Haibo Zeng, Weiping Cai, Yue Li, Jinlian Hu, and Peisheng Liu. *Composition/Structural Evolution and Optical Properties of ZnO/Zn Nanoparticles by Laser Ablation in Liquid Media.* J. Phys. Chem. B, **109**, (2005), pp. 18260–18266.
11. P. F. Carcia, R. S. McLean, M. H. Reilly, and G. Nunes Jr. *Transparent ZnO thin-film transistor fabricated by RF magnetron sputtering.* Appl. Phys. Lett. **82**, (2003), **1117**.
12. X. W. Sun, and H. S. Kwok. *Optical properties of epitaxially grown zinc oxide films on sapphire by pulsed laser deposition.* J. Appl. Phys. **86**, (1999), **408**.
13. T Schuler, and M.A Aegerter. *Optical, electrical and structural properties of sol gel ZnO:Al coatings*. Thin Solid Films, **351**, (1999), pp. 125–131.
14. Ruoyu Hong, Tingting Pan, Jianzhong Qian, and Hongzhong Li. *Synthesis and surface modification of ZnO nanoparticles.* Chemical Engineering Journal, **119**, (2006), pp. 71–81.
15. M. Hjiri, L. El Mir, S.G. Leonardi, A. Pistone, L. Mavilia, and G. Neri. *Al-doped ZnO for highly sensitive CO gas sensors.* Sensor and Actuators B **196** (2014), pp. 413-420.
16. X.B. Li, Q.Q. Zhang, S.Y. Ma, G.X. Wan, F.M. Li, and X.L. Xu. *Microstructure optimization and gas sensing improvement of ZnO spherical structure through yttrium doping.* Sensor and Actuators B **195** (2014), pp. 256-533.
17. Chang Chun Chen, Ping Liu, and Chun Hua Lu. *Synthesis and characterization of nano-size ZnO powders by direct precipitation method.* Chemical Engineering Journal, **144**, (2006), pp. 509-513.
18. A. M. Pineda, R. Herrera-Rivera and, M. de la L. Olvera. *Synthesis and Characterization of ZnO Powders by Homogeneous Precipitation from Different Precursors*. 2014 11th International Conference on Electrical Engineering, Computing Science and Automatic Control (CCE). 978-1-4799-6230-3/14/$31.00 ©2014 IEEE
19. Jiaheng Wang, Yang Qi, Zhuangzhi Zhi, Jing Guo, Maolin Li, and Ying Zhang. *A self-assembly mechanism for sol-gel derived ZnO thin films*. Smart Materials and Structures IOP Publishing, **16**, (2007) pp. 2673-2679.